Frequent Seismic Monitoring of Carbon Dioxide Injection: The Advantage of Using Onset Times for Reservoir Characterization and Monitoring

D. W. Vasco, Lawrence Berkeley National Laboratory, Andrey Bakulin, EXPEC Advanced Research Center, Saudi Aramco

Downloaded 10/22/17 to 166.87.199.141. Redistribution subject to SEG license or copyright; see Terms of Use at http://library.seg.org/

Summary

The onset time, the time at which a geophysical observation begins to change from its background value, is a very useful attribute for reservoir characterization. In particular, the onset time has a robust relationship to flow and flow properties in the reservoir even in the presence of uncertainty as to which rock physics model is appropriate. We illustrate this by a numerical simulation involving the monitoring of injected carbon dioxide.

Introduction

A serious deficiency of many current monitoring programs is that the time intervals between follow-up surveys is very large, typically a year or more, resulting in significant sampling aliasing of reservoir processes. Therefore, it is difficult to differentiate between temporal variations in seismic data due to saturation changes, pressure changes, and deformation. This may change with the increasing use of permanent sensors for frequent long-term monitoring. With better temporal sampling one can try to disentangle the various factors leading to changes in seismic observations over time. Here we illustrate the advantages associated with monitoring the changes in seismic properties of a reservoir on a regular, even semi-continuous, basis. In particular, we show that the use of onset times, the time at which a geophysical attribute changes, can be of some advantage in relating seismic time-lapse changes to flow within the reservoir. For example, the onset time is a robust property in the face of the uncertain relationship between the fluid distribution and the effective seismic velocity noted below.

CO_2 rock physics challenges

The injection of carbon dioxide within a reservoir has consequences for its seismic reflectivity. Unfortunately, the relationship between the presence of carbon dioxide, or any fluid for that matter, and reservoir reflectivity is not always straightforward. In fact, the seismic velocity change associated with a given saturation change is complicated by a number of factors that are still the subject of some debate. The seismic velocity and its frequency dependence (dispersion) and corresponding attenuation are influenced by fluids in the porous rock via a number of physical mechanisms. The seismic response may depend upon the small-scale fluid distribution within a reservoir. We should note that there are a number of other mechanisms influencing seismic velocity, particularly with regard to the chemical effects of carbon dioxide on the rock matrix (Vanorio et al., 2010; Ghosh and Sen, 2012).

Method

In this section we illustrate the advantages of using seismic onset times for reservoir characterization by way of a numerical example. We use bounds to capture the range of uncertainty in effective seismic velocity due to a specific volumetric fluid composition. Then we compare estimates of amplitude changes due to fluid saturation changes to estimates of onset times.

Given the rock physics challenges noted above, it is probable that our assumed relationships between the fluid saturations and seismic velocity, and ultimately seismic amplitude, are in error to some degree. To examine the influence of assuming an incorrect model we consider upper and lower bounds on the possible velocities for a given saturation of carbon dioxide. In this study we use the Voigt-Reuss bounds, also known as the harmonic and arithmetic averages (Mavko et al., 1998) to represent the extreme variation that is possible in relating the saturation of carbon dioxide to seismic compressional velocity. The Voigt upper bound for the bulk moduli of a mixture of fluids is given by

$$K_V = \sum_{i=1}^{3} f_i K_i,$$

where f_i is the volume fraction of the i-th fluid and K_i is the bulk modulus of the i-th fluid. This upper bound is obtained when all the contributing components are arranged in parallel. One can visualize this as layers of pure components arranged parallel to the direction of propagation. Then some portion of an elastic wave may propagate solely within the fastest layer. The Reuss lower bound for the effective fluid bulk modulus is given by

$$\frac{1}{K_R} = \sum_{i=1}^{3} \frac{f_i}{K_i}.$$

The lower bound is obtained when all the components are arranged in series. This can be pictured as propagation in a direction perpendicular to layers of pure components. Hence, a propagating wave must traverse the volume fraction of the slowest material. The Voigt-Reuss bounds are plotted in Figure 1 along with the estimate of Hill (1963) which is the average of the Voigt and Reuss bounds.

Other bounds, such as the Hashin-Shtrikman bounds (Hashin and Shtrikman, 1963), are possible but the Voigt-

© 2013 SEG

DOI http://dx.doi.org/10.1190/segam2013-0304.1

Downloaded 10/22/17 to 166.87.199.141. Redistribution subject to SEG license or copyright; see Terms of Use at http://library.seg.org/

Reuss bounds are the simplest and the most conservative range of possible velocities for a particular volumetric mixture of fluid saturations. For example, the Voigt-Reuss bounds are valid in the presence of anisotropy while the Hashin-Shtrikman bounds are only valid for a macroscopically homogeneous and isotropic material.

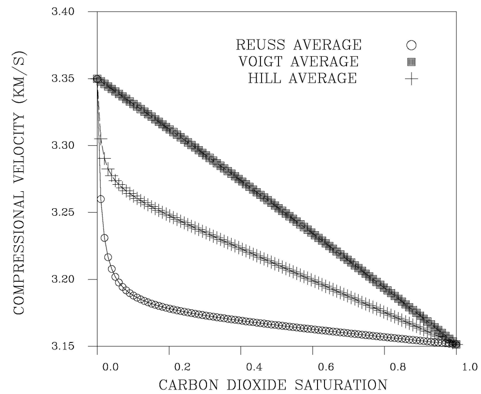

Figure 1. Reuss, Voigt, and Hill velocities associated with variable carbon dioxide saturation in the reservoir.

For the conditions and the frequency range of this simulation, Gassmann's approach for computing the elastic moduli is an adequate approximation. The effective bulk moduli of the entire saturated rock, K_{sat}, including the three fluids water, oil, and carbon dioxide, and the properties of the rock constituents or grains and the frame moduli is given by Gassmann's (1951) relation

$$K_{sat} = K_{dry} + \frac{\left(1 - K_{dry}/K_{grain}\right)^2}{\phi / K_{fluid} + (1-\phi)/K_{grain} + K_{dry}/K_{grain}^2},$$

where K_{dry} is the dry frame bulk modulus, K_{grain} is the bulk modulus of the solid grains comprising the rock, K_{fluid} is the fluid bulk modulus given by either the Voigt, Reuss, or Hill moduli mentioned above. For a particular elastic overburden model, and a poroelastic reservoir model, we can compute the seismic response as a function of the changing reservoir conditions. In this example we will assume that the pressure effects on seismic velocity are insignificant and will only consider amplitude changes due to saturation changes. We will consider near-offset reflection amplitudes and we shall assume that the reservoir model consists of cells of significant lateral dimensions, say a hundred meters or more. Therefore, for the sake of this numerical simulation, we will represent the reservoir and the surrounding medium by a collection of one-dimensional columns. The location of the layer boundaries of the column approximate the depths of the reservoir layers at that particular location. Each column may have a distinct set of fluid saturations as in Vasco et al. (2004).

Synthetic case study: CO2 injection

Consider the model shown in Figure 2, where the permeability varies over three orders of magnitude. Higher permeabilities lie to the north and west of a central injection well, denoted by a circle in the center of the plot. The lowest permeabilities are to the south of the injector. The reservoir model is a 10 by 10 grid of cells in two layers, giving cell dimensions of 150 by 150 m. The two layers are 46 and 64 m thick, respectively. The central well is injecting carbon dioxide into a layer saturated with 90 percent water and 10 percent oil.

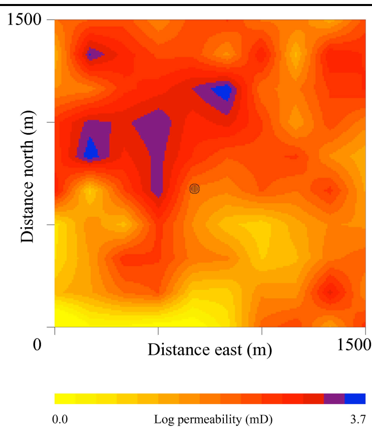

Figure 2. Reference permeability model. The injection well is indicated by the central filled circle.

As noted previously, for a given combination of fluid volumes or saturations within a given cell, there are numerous ways to compute an effective fluid modulus, depending upon the particular distribution of fluid within the cell. For example, the fluid may be distributed in a relatively homogeneous fashion or it may reside in patchy islands of one fluid embedded within the porous medium comprising the cell. In addition, the fluid may be distributed in an anisotropic manner due to variations in flow properties. As noted above, the Reuss lower bound and the Voigt upper bound represent the range of possible bulk moduli given a particular volume fraction of fluids. In Figure 1 we plot the Reuss and Voigt velocity, obtained by using the respective moduli as a function of the saturation of carbon dioxide. The estimate of Hill (1963) which is the average of the two bounds is also shown. For a given saturation, the two bounds predict very different velocities except at the end points. Furthermore, the variation of compressional velocity with fluid saturation is dramatically different. The Voigt velocity decreases almost linearly with saturation whereas the Reuss velocity decreases sharply as carbon dioxide is introduced but then flattens out.

© 2013 SEG

DOI http://dx.doi.org/10.1190/segam2013-0304.1

Downloaded 10/22/17 to 166.87.199.141. Redistribution subject to SEG license or copyright; see Terms of Use at http://library.seg.org/

Embedding the two layer reservoir model in an elastic half space we can use Kennett's (1983) method and Gassmann's equations to compute the amplitude changes due to the saturation changes. Both the Reuss and Voigt estimates were used to calculate the moduli leading to the amplitude changes shown in Figure 3. Both the magnitude and the distribution of amplitudes change significantly if one changes the method for computing the fluid bulk moduli. This will have important consequences if one tries to use the amplitude changes to estimate fluid saturation changes and then flow properties.

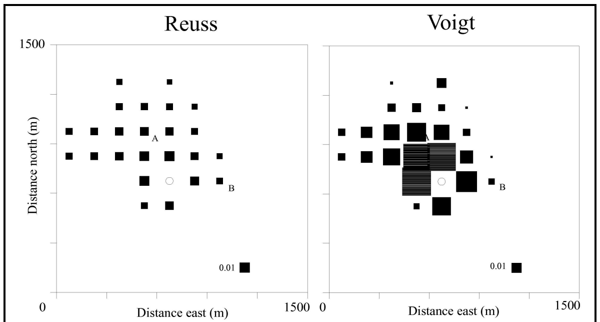

Figure 3. Amplitude change computed by Reuss and Voigt averages. The amplitude changes are between surveys at 3600 and 100 days from the start of injection.

To gain some insight into the amplitude changes due to the injection of carbon dioxide, let us consider a point, labeled A in Figure 3, and follow the relative amplitude changes as the injection proceeds. In the examples that follow we simulate 50 seismic monitoring surveys over the total time interval of 3600 days with the first survey beginning 100 days after the start of injection. This results in an estimate of the seismic amplitudes every 70 days. In Figure 4 we plot the relative change in amplitude, which is the amplitude change at a given time normalized by the original amplitude.

Because the background velocity estimates are different for the Reuss and Voigt approaches, the normalization amplitude differs for each estimate. That is why the two curves do not trend to the same value. Note how the curves vary significantly as a function of time and even cross over at around 1500 days. As expected, the Reuss average decreased rapidly after the saturation front reaches the point then changes much more slowly with time. The Voigt velocity estimate decreases at a fairly steady rate with time. Consequently, both curves start to decrease at the same time, roughly 700 days, the time at which the fluid saturations begin to change.

From an examination of the curves in Figure 4, it seems that the time at which the amplitudes begin to change, the "onset time", appears to be independent of the method used to obtain the compressional velocity and ultimately, an amplitude change. We can verify this by computing the onset time for all of the amplitude estimation points used in Figure 3. The resulting onset times, based upon both the Reuss and Voigt estimates, are shown in Figure 5. The two sets of onset times appear to be very similar, in stark contrast to the amplitude changes shown in Figure 3.

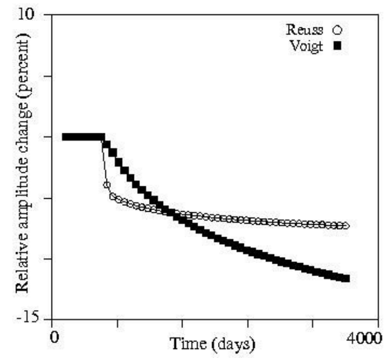

Figure 4. Amplitude change computed by Reuss and Voigt averages for point A in Figure 3.

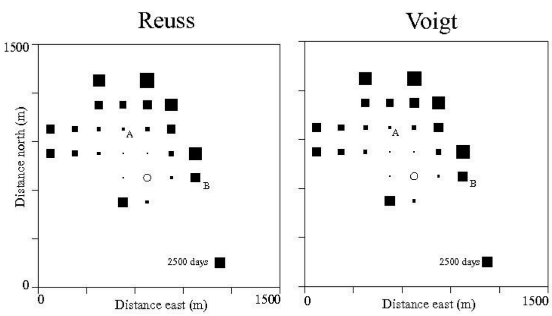

Figure 5. Onset times computed from the Reuss and Voigt averages.

Permeability inversion

As an illustration of the value of onset times for reservoir characterization, consider the results of two sets of time-lapse permeability inversions. We start with a simple homogeneous layered permeability model and in a complete closed loop comprised of reservoir and seismic simulation we attempt to match a time-lapse behavior of a particular seismic attribute from all 50 repeat surveys. The algorithm is an iterative linearized solution of the nonlinear inverse problem with streamline sensitivities, as described in Vasco et al. (2004). One set of inversions utilizes time-lapse amplitude changes as the underlying seismic attribute, while the other set is based upon onset times. For each set, the Hill, the Reuss, and the Voigt algorithms are used to compute seismic velocity changes from the reservoir simulation but the Hill approach is used to compute the

DOI http://dx.doi.org/10.1190/segam2013-0304.1

Downloaded 10/22/17 to 166.87.199.141. Redistribution subject to SEG license or copyright; see Terms of Use at http://library.seg.org/

sensitivities and the residuals for the inversion. The convergence as a function of the number of iterations are shown in Figure 6 for the two sets of inversions. The inversions of amplitude changes generally do not converge

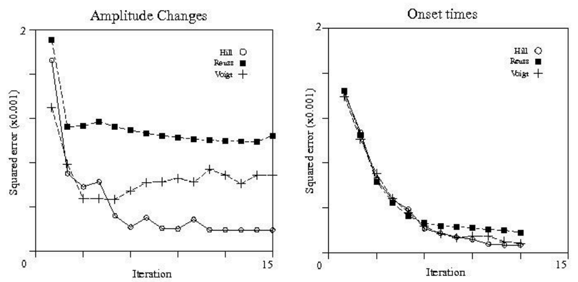

Figure 6. Squared errors as a function of iteration for amplitude (left) and onset time inversions (right).

to small total errors if the relationship between fluid content and seismic velocity is in error. Onset time inversions, on the other hand, do produce significant error reductions even when the relationship is in error. Furthermore, as evident in Figures 7 and 8, the amplitude inversions may not recover the resolved permeability field if the relationship between seismic velocity and fluid saturation is incorrect. Onset time inversions are more stable, recovering the general permeability distribution even when the rock physics relationship is in error (Figure 8).

Conclusions

The results of this and previous studies suggest that amplitudes may be used to infer flow properties in a reservoir if the relationship between saturation and seismic velocity is well constrained. However, given uncertainty in the mapping between fluid saturation and seismic velocity, the results of an amplitude inversion may be in error. Our results indicate that a better attribute to extract from the time-lapse data is the onset time, the time at which a seismic observation begin to deviate from its initial background value. Onset times appear to be more stable with respect to variations in the relationship between fluid saturations and seismic velocities and amplitudes. For this reason, onset times may provide a more robust basis for reservoir monitoring and characterization. In practice, the onset time will signify when a seismic observation, such as an amplitude change, exceeds the background noise level. Thus, there may be a delay between the time at which a physical quantity begins to change and the time at which the change exceeds the background noise. Therefore, it may make sense to reference the onset time to changes directly above the injection well, rather then to the start of injection. The use of onset times is particularly well suited for long term monitoring using frequent surveys and permanently installed seismic sensors.

Onset times can be produced with frequent time-lapse monitoring of reservoir operations. The technology for frequent time-lapse monitoring is advancing or has advanced in particular areas of geophysics. New approaches for frequent seismic monitoring have appeared recently. For example, permanently deployed shallow seismic sensors are being tested for frequent monitoring of the injection of carbon dioxide (Bakulin et al., 2012). Continuous active source monitoring is being developed in a variety of settings, including cross-well and vertical seismic profiling configurations, for the monitoring of fluid movement within the subsurface (Daley et al. 2007).

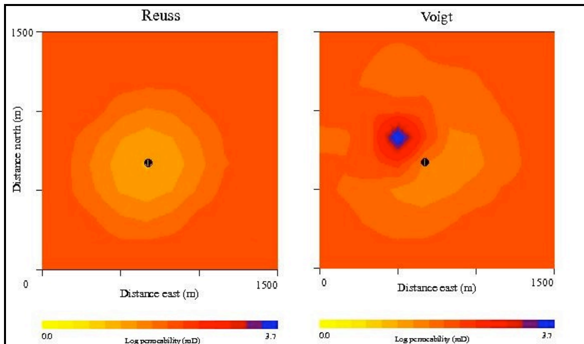

Figure 7. Inversion results for Reuss and Voigt amplitude changes.

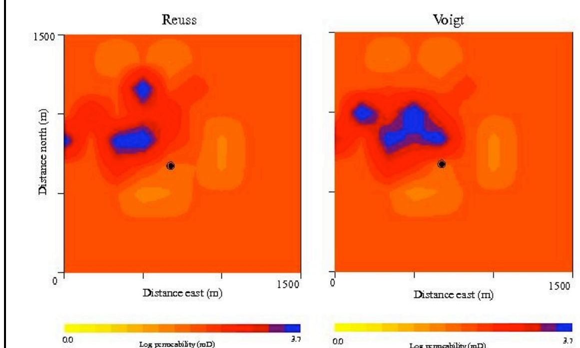

Figure 8. Inversion results for Reuss and Voigt onset times.

Acknowledgments

This work was supported by the EXPEC Advanced Research Center of Saudi Aramco and by the US Department of Energy under contract number DE-AC02-05-CH11231, Office of Basic Energy Sciences, and the GEOSEQ project for the Assistant Secretary for Fossil Energy, Office of Coal and Power Systems, through the National Energy Technology Laboratory of the US DOE.

© 2013 SEG

DOI http://dx.doi.org/10.1190/segam2013-0304.1

http://dx.doi.org/10.1190/segam2013-0304.1

EDITED REFERENCES

Note: This reference list is a copy-edited version of the reference list submitted by the author. Reference lists for the 2013 SEG Technical Program Expanded Abstracts have been copy edited so that references provided with the online metadata for each paper will achieve a high degree of linking to cited sources that appear on the Web.

REFERENCES

Bakulin, A., R. Burnstad, M. Jervis, and P. Kelamis, 2012, Evaluating permanent seismic monitoring with shallow buried sensors in a desert environment: 82nd Annual International Meeting, SEG, Expanded Abstracts, doi:10.1190/segam2012-0951.1.

Daley, T. M., R. D. Solbau, J. B. Ajo-Franklin, and S. M. Benson, 2007, Continuous active-source seismic monitoring of CO_2 injection in a brine aquifer: Geophysics, **72**, no. 5, A57–A61, http://dx.doi.org/10.1190/1.2754716.

Gassmann, F., 1951, Über die elastizität poröser medien: Vierteljahrsschrift der Naturforschenden Gesellschaft in Zurich, **96**, 1–23.

Ghosh, R., and M. K. Sen, 2012, Predicting subsurface CO_2 movement: From laboratory to field scale: Geophysics, **77**, no. 3, M27–M37, http://dx.doi.org/10.1190/geo2011-0224.1.

Hashin, Z., and S. Shtrikman, 1963, A variational approach to the elastic behaviour of multiphase materials: Journal of the Mechanics and Physics of Solids, **11**, no. 2, 127–140, http://dx.doi.org/10.1016/0022-5096(63)90060-7.

Hill, R., 1963, Elastic properties of reinforced solids: Some theoretical principles: Journal of the Mechanics and Physics of Solids, **11**, no. 5, 357–372, http://dx.doi.org/10.1016/0022-5096(63)90036-X.

Kennett, B. L. N., 1983, Seismic wave propagation in stratified media: Cambridge University Press.

Mavko, G., T. Mukerji, and J. Dvorkin, 1998, The rock physics handbook: Cambridge University Press.

Vanorio, T., G. Mavko, S. Vialle, and K. Spratt, 2010, The rock physics basis for 4D seismic monitoring of CO_2 fate: Are we there yet?: The Leading Edge, **29**, 156–162, http://dx.doi.org/10.1190/1.3304818.

Vasco, D. W., A. Datta-Gupta, R. Behrens, P. Condon, and J. Rickett, 2004, Seismic imaging of reservoir flow properties: Time-lapse amplitude changes: Geophysics, **69**, 1425–1442, http://dx.doi.org/10.1190/1.1836817.

Downloaded 10/22/17 to 166.87.199.141. Redistribution subject to SEG license or copyright; see Terms of Use at http://library.seg.org/